Light Metals 2011 *Edited by: Stephen J. Lindsay*
TMS (The Minerals, Metals & Materials Society), 2011

Light Metals 2011

ALUMINUM REDUCTION TECHNOLOGY

Cells Thermal Balance

SESSION CHAIR
Bernard Allais
Rio Tinto Alcan
France

Light Metals 2011 *Edited by: Stephen J. Lindsay*
TMS (The Minerals, Metals & Materials Society), 2011

INCREASING THE POWER MODULATION WINDOW OF ALUMINIUM SMELTER POTS WITH SHELL HEAT EXCHANGER TECHNOLOGY

Pascal Lavoie[1], Sankar Namboothiri[1], Mark Dorreen[1], John JJ Chen[1], Donald P Zeigler[2] and Mark P Taylor[1]
[1]Light Metals Research Centre, The University of Auckland, Private Bag 92019 Auckland, New Zealand
[2]Alcoa Primary Metals, Aluminerie Deschambault, 1 Boul. Des Sources, Qc, Canada, G0A 1S0

Keywords: power modulation, shell heat exchanger, sidewall heat transfer

Abstract

With power prices constantly rising, and varying aluminium prices requiring operating flexibility, the financial incentive for smelters to adopt a power modulation strategy is becoming larger. However, the power modulation window, in which a smelter can safely operate its reduction cells, is limited. The Light Metals Research Centre has developed the Shell Heat Exchanger (SHE) technology for controlling the heat dissipation from aluminium smelting pot shells. By varying the air flow through the SHE, the heat removal from the shell can be increased or decreased as desired, doubling the previous power modulation window or allowing power modulation with minimal disturbance to the pot thermal balance.

This paper presents experimental results from LMRC's test facility, which show the shell temperature response when the SHE is operated in cooling or insulating mode. Steady state thermo-electric model results for these operating scenarios are also presented, outlining the impact on ledge thickness and other pot operating conditions.

Introduction

Need for Power Modulation

A continuous increase in energy cost is changing the cost structure of smelters. Previously, energy accounted for less than 30% of production costs, recent figures show it amounts to 40%, or more in many smelters [1]. This forces smelters to change their operating strategy by finding alternative ways to reduce energy consumption in order to remain financially viable. Reducing the anode-cathode distance is a mechanism of choice, helped by the re-emergence of drained and other cathode technologies, especially in China [2]. Another mitigating strategy increasingly being considered and implemented is power modulation. This is mostly advantageous for plants requiring the acquisition of electricity on the spot market where a large shift in price is observed on a daily, or other periodic basis, or those able to obtain better contractual rates by agreeing to modulation. Figure 1 shows spot price on the European market for the week of September 6, 2010 [3].

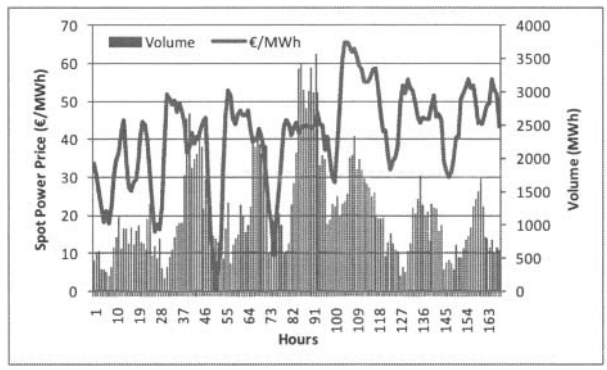

Figure 1. EEX hourly power price and volume for the week of September 6 2010

Effect of Power Modulation on Cell Operations

As described by Eisma and Patel [4], the dynamic response of the electrolysis cell to a reduction of 10 to 12% in power input starts with a sudden drop in temperature, followed by a linear drop in both temperature and liquidus over the following 24 hours, resulting in ledge freeze and reduction in liquid bath volume. It was also noted that the dynamic response returning to the original power input was slower, in regards to ledge melting and bath volume.

The long term effects of power modulations on the electrolysis cells can be quite damaging. Operating a power modulation scheme over extended periods can lead to severe damage of cathodes due to the solidification of sludge on the surface following the mechanisms described by Taylor et al if the surface temperature remains below 945 to 950°C [5]. However, with adequate understanding of the dynamic heat balance of the cell and proper adjustment to the modulation scheme, day-night cycles of up to 10% power (amperage) variation can be operated indefinitely without observable damage to cathodes. In any case, the power modulation window, i.e. the range of power inputs where a given cell will operate sustainably, is very limited by the heat loss rate of cells, and their re-heating characteristics.

Increasing the Power Modulation Window with Shell Heat Exchangers

Power modulation introduces the opposite thermal challenge compared to capacity creep. In modulation the heat balance must be altered to either increase the heat generation or decrease dissipation to avoid excessive ledge freeze. By varying the heat dissipation from the pot shell, it is possible to adjust the dynamic

response of the pot to a change in power input, thereby enabling a larger power modulation window.

The Light Metals Research Centre (LMRC) at the University of Auckland has developed a technology capable of providing both controlled cooling and insulation to sidewalls using heat exchangers, installed on-line, with variable air flow. Moreover, the hot air from the heat exchangers is collected and removed from the potroom. The heat content of the air at 150-200°C can be recovered and re-used in various low grade thermal applications including desalination and refrigeration. The performance of LMRC Shell Heat Exchanger (SHE) using compressed air was previously published along with its potential application during capacity creep [6]. The present paper reports the performance of SHE powered using an extraction fan and fitted to the sidewall of a full scale cell demonstration model. The expected benefits of power modulation for smelters from SHE technology are also discussed using 3D thermo-electric modelling of a mid-range amperage reduction cell.

Experimental

Shell Heat Exchangers

Figure 2 shows a schematic of one of the SHE designs developed by LMRC. The shell heat exchanger is comprised of two parts; an exchanger body and an exchanger inlet and outlet. The exchanger body incorporates vortex generators (not shown in the Figure) to enhance the heat transfer. None of the other cell heat exchangers reported to date has made use of turbulence promoters to increase the heat transfer rate. Although shell fins are used extensively to increase heat dissipation by increasing the transfer surface, they can restrict convective flow on the shell face and reduce radiative heat transfer by reflecting to each other at higher temperatures. The SHE however, makes use of proprietary turbulence promoters which increase the heat transfer rate when compared with the rates calculated using standard engineering design equations. More details are given below.

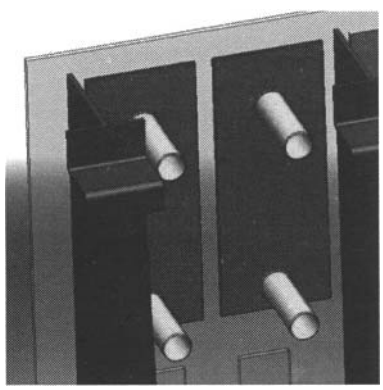

Figure 2. Schematic of Shell Heat Exchangers (SHE) in the demonstration model inter-cradle spacing

Figure 3 illustrates in broad terms the mode of operation of extraction fan powered SHEs. The vacuum generated by the fan draws air into the shell heat exchanger inlet from the outside vicinity. The air flows up the gap between the steel shell and the heat exchanger and then exits via the opening at the top of the exchanger into the extraction duct which is connected to the fan. The cell wall is cooled while the exchanger air is heated. The alternate SHE model, driven by a blowing device (such as compressed air or powered fan) produces similar heat transfer. These SHE options have been plant tested and the choice of suction or blowing mode should be based on specific smelter design and operating considerations such as cost of installation.

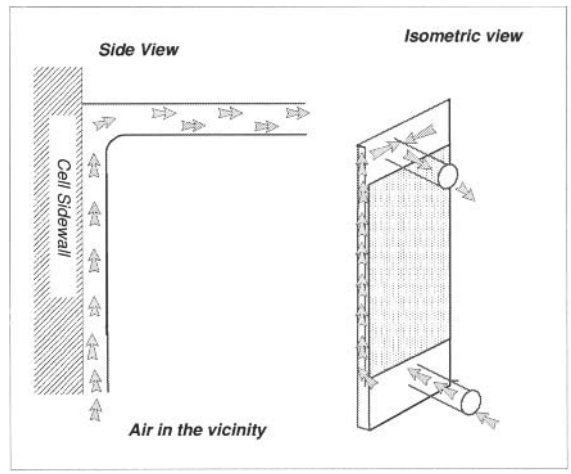

Figure 3. SHE operation showing air flow path

Sidewall cooling Demonstration Facility

The details of the LMRC sidewall cooling demonstration models were discussed previously [6]. The facilities essentially represent two 3-cradle pot shells of 350 kA technology facing each other. The sidewalls are heated by electrical elements mounted inside the sidewall and are thermally insulated on the inner sidewall face to ensure almost all heat flows through the shell.

Experimental Procedure

Four shell heat exchangers, (two of 140 mm wide and two of 95 mm wide) were mounted to the central inter-cradle space on one pot shell. This has given 77% area coverage of the shell within the inter-cradle space. Air flow through the exchangers was powered by a centrifugal fan located outside the demonstration model. Ducting from the fan was fitted to the exchanger outlets to provide the suction and remove the hot air. Figure 4 shows the actual arrangement of SHEs mounted on the central inter-cradle space of the demonstration model.

Figure 4. SHEs mounted using a simple one-piece hanger in central inter-cradle space of the demonstration model

The pot shell was initially heated to a steady state temperature with zero air flow through the SHEs. Once the required temperature was attained on the shell, air was admitted through the SHEs to cool the central inter-cradle space and the same flow rate was maintained until a new steady state value was attained. Figure 5 shows a typical shell temperature recording of the experiment. The following parameters were recorded during the experiments:

- Temperature at various locations on the inter-cradle space with and without SHEs.
- Flow rate, pressure and temperature of the extracted air, measured at the fan exhaust.
- Velocity and temperature of the hot exit air from the SHEs (measured in the duct, approximately 1 m from the exit of SHEs).
- Ambient temperature

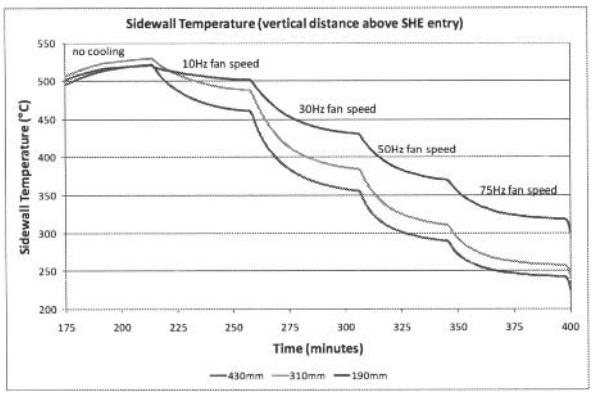

Figure 5. Typical shell temperature record from an experiment

Results

Figure 6 compares the shell vertical temperature profile at various air flow rates with and without SHEs installed while Figure 7 shows the corresponding temperature reduction. When no forced air extraction is applied to SHEs (0 scfm), they act as insulators, locally increasing the average shell temperature by up to 75°C. When cooling was applied, a peak sidewall temperature reduction of up to 200°C was obtained in this case. The sidewall cooling was controlled by adjusting the extraction fan speed. The temperature of the air measured at 1 m from the outlet of the SHEs was between 170 to 200°C. This corresponds to a heat content of 9-10 kW per cradle position.

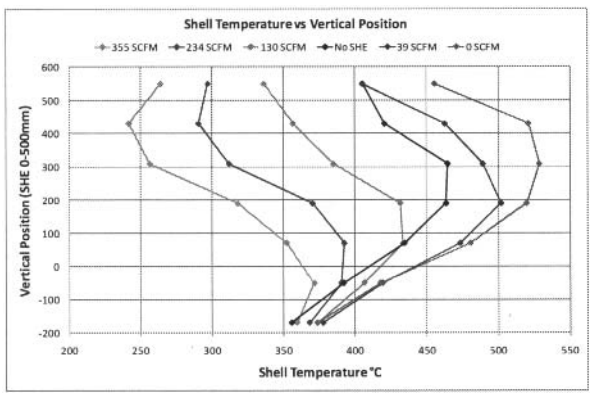

Figure 6. Vertical temperature profiles at various air flow

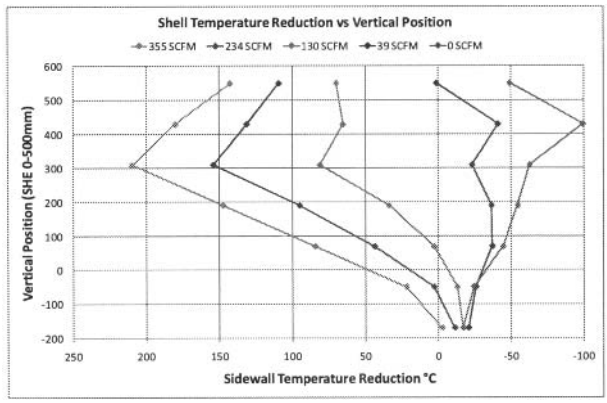

Figure 7. Temperature reduction profile at various air flows

Shell to Air Heat Transfer Coefficient

The shell to air heat transfer coefficient is an important parameter in the sidewall heat transfer circuit as it dictates the overall sidewall heat flow and hence the ledge thickness of high amperage aluminium cells. The effective shell to air heat transfer coefficient ranges from 25 to 30 W/m^2.K for a typical pot shell approaching 350°C [7]. The LMRC shell heat exchanger, depending on the air flow, alters the shell to air heat transfer coefficient to adjust the sidewall heat flow.

The effective shell to air heat transfer coefficient for the SHE was calculated for various air flow rates by Equation (1). This is based on the heat gained by the exit air from the shell heat exchanger and considering only the shell surface covered by the shell heat exchanger as the heat transfer area.

$$h = \frac{\Delta Q}{A T_{LMTD}} \quad (1)$$

Where h is effective heat transfer coefficient from shell to air, W/m^2.K

ΔQ is the heat content of the exit air, W

A is the area of the shell surface covered by the shell heat exchanger, m^2

T_{LMTD} is the logarithmic mean temperature difference of the shell heat exchanger, K

Prediction of the forced convection heat transfer coefficient was also made using the Sieder Tate equation [8] applied for a rectangular duct of the same dimensions as the shell heat exchanger. The Sieder Tate equation is:

$$\frac{hD_e}{K} = 0.023\left(\frac{D_e V \rho}{\mu}\right)^{0.8}\left(\frac{C_p \mu}{K}\right)^{0.33} \quad (2)$$

Where h is the effective heat transfer coefficient from shell to air, W/m^2.K

D_e is the equivalent diameter of a rectangular duct of same dimension as the shell heat exchanger, m

V is the superficial air velocity inside the duct , m/s

*ρ is the density of air, kg/m^3

*μ is the viscosity of air, kg/m.s
*C_p is the specific heat capacity of air, J/kg.K
*K is the thermal conductivity of air, W/m.K

** calculated at mean air temperature inside the rectangular duct*

Figure 8 shows the heat transfer coefficient at different air flow rates (air flow quoted per cradle position of the demonstration model). The overall heat transfer coefficient increased with increasing flow rate. Note that the heat transfer coefficients measured for the SHE are 1.5 to 2.5 times higher than that predicted for forced convection through a duct of same dimensions. This increase is due to turbulent promoters mentioned earlier. The increase in heat transfer coefficient compared to forced convection is consistent with the previous findings [9, 10].

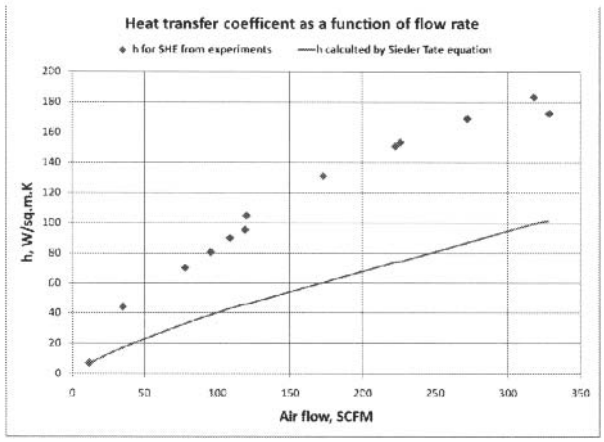

Figure 8. SHE effective heat transfer coefficients as a function of air flow rate

To determine an approximate value for effective shell to air heat transfer coefficient in insulation mode, experiments were conducted by supplying a small but measurable amount of air to the shell heat exchanger (10 SCFM per cradle position). This small amount of air supplied did not change the vertical temperature profile from a no-flow situation. The effective heat transfer coefficient under this condition was calculated using Equation (1) and found to be between 7 and 10 W/m^2.K (as shown in Figure 8).

Thermo-electric modelling

A thermo-electric 3D slice model of a mid-amperage cell was built to illustrate how the heat balance of a cell can be manipulated by controlling the heat transfer coefficient at the shell to increase the power modulation window. Although the steady-state nature of the model does not show the short term dynamic response of the cell (in the first few hours), it has proved useful in indicating the effect of SHE operation on the sidewall heat flow and ledge thickness over a number of days.

Taking a base case where the cell would normally operate at 222kA, with a voltage of 4.36V, alternative cases were ran at 200kA and 240kA, both at increased ACD, with and without SHE. Various heat transfer coefficient inside the exchanger were applied. In the first case 80 and 150 W/m^2.K were used to represent different air flow situations. In the second case 10 W/m^2.K was used to represent an insulating, minimum flow situation. Two SHE sizes were also modelled, representing 25% and 80% surface coverage of the pot side shell (above the cathode surface level).

Modelling results

The key inputs and outputs of the model are shown in Table I and the predicted ledge profile in Figure 9.

Table I. Key modelling input and output

KEY INPUTS	Base Case	BC1	BC1_001	BC1_002	BC2	BC2_001	BC2_002
Line Current (kA)	222	240	240	240	200	200	200
ACD (cm)	4.14	4	4	4	4.82	4.82	4.82
Liquidus (°C)	948	948	948	948	948	948	948
SHE coverage (%)	0	0	25%	25%	0	25%	80%
HTC in SHE (W/sq.m.k)	35	35	80	150	35	10	10
KEY OUTPUTS	**Base Case**	**BC1**	**BC1_001**	**BC1_002**	**BC2**	**BC2_001**	**BC2_002**
Avg Bath Temp (°C)	958.2	964	961.9	962.2	954.4	954.8	954.7
Superheat (°C)	10.2	16	13.9	14.2	6.4	6.8	6.7
Avg Shell Side Temp (°C)	319	404.1	329.3	274	259.9	288.7	382.3
Max Shell Side Temp (°C)	471.7	638.1	515	429.4	381.4	435	568.1
Avg Shell Bottom Temp (°C)	159.6	162.3	161.2	160.5	157.4	157.8	158.9
Avg Cover Surface Temp (°C)	331.8	340.4	339.9	340	321	321.3	321.5
Ledge Pinch Point (cm)	3.4	0.7	1.6	2.1	9.5	7.8	3.8
VOLTAGE BREAKDOWN	**Base Case**	**BC1**	**BC1_001**	**BC1_002**	**BC2**	**BC2_001**	**BC2_002**
Cell EMF	1.76	1.76	1.76	1.76	1.76	1.76	1.76
Anode V Drop	0.544	0.593	0.592	0.593	0.482	0.395	0.481
Bath V Drop (Including EMF)	3.315	3.389	3.392	3.395	3.363	3.460	3.370
Cathode V Drop	0.491	0.528	0.529	0.53	0.443	0.414	0.443
Model Voltage (Excl. extern.)	4.350	4.51	4.513	4.518	4.288	4.269	4.294
HEAT GENERATION	**Base Case**	**BC1**	**BC1_001**	**BC1_002**	**BC2**	**BC2_001**	**BC2_002**
Reaction Voltage (V)	2.022	2.022	2.022	2.022	2.022	2.022	2.022
Ohmic Generation (V)	2.328	2.488	2.491	2.496	2.266	2.247	2.272
Heat Generated (kW)	**516.8**	**597.1**	**597.8**	**599.0**	**453.2**	**449.4**	**454.4**
HEAT LOSSES (kW)							
Loss Rod/Yoke	61.6	65.7	65.6	65.6	56.9	56.9	56.4
Loss Cover	173.4	187.5	182.6	178.6	159.4	161.3	169.1
Total Loss Shell	215.9	271.4	278.5	285.1	177.5	175.9	167.4
Loss Shell Side	174.5	229.0	236.6	243.4	137.0	135.2	126.3
Loss Shell Bottom	41.4	42.4	42.0	41.7	40.6	40.7	41.1
Loss Collector Bars	61.9	68.4	66.6	65.2	54.5	55.2	60.8
Total Heat Loss (kW)	**512.8**	**593.0**	**593.4**	**594.5**	**448.4**	**449.3**	**453.7**

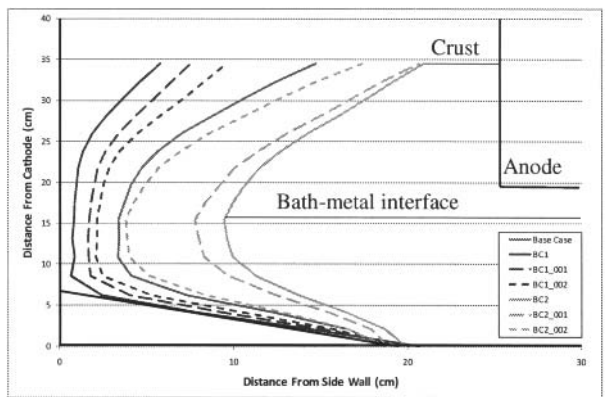

Figure 9. Predicted ledge profile at different amperage and SHE heat transfer coefficient and coverage.

Effects on the Heat Balance and Increase in Modulation Window

It can be seen that the use of heat exchangers at low flow partially mitigates the increase in shell temperature caused by the higher power input in the cell, while providing an increase in ledge thickness (BC1 and BC1_001). The redistribution of the heat balance, the increase in ledge thickness and the reduction in

superheat offer an opportunity to increase the amperage further. Increasing the heat transfer coefficient in the SHE to 150 W/m^2.K (BC1_002) results in a further increase in ledge thickness.

Simulating the opposite situation, where the power input to the cell is reduced by 22 kA with an increase in ACD (BC2), the ledge pinch point increases to 9.5 cm and the superheat is reduced to 6.4°C. Introducing the SHE with a heat transfer coefficient of 10 W/m^2.K (BC2_001) results in a small increase in superheat (0.4°C) and a retraction of the ledge, especially at the pinch point (-1.7 cm). It is important to note that the top of the ledge remains unchanged, contacting the anode side.

Unlike the higher amperage case, a further reduction of the heat transfer coefficient is difficult without endangering the SHE in its present configuration. However, the heat transfer through the side can be further limited by increasing the surface coverage of the heat exchangers (BC2_002). This results in the ledge retracting almost to the Base Case position, effectively doubling the power modulation window on the low side to a reduction of 40kA. Higher SHE coverage would also increase the heat recovery potential, requiring lower flow for a given cooling at high amperage and increasing heat grade.

Note that in all cases, the heat balance is adjusted mostly between the sides and the top of the cell, leaving the ledge position on the cathode surface without significant changes.

Figures 10, 11 and 12 show the predicted impact of the shell heat exchangers on the sidewall heat flux, the bath superheat and the ledge thickness.

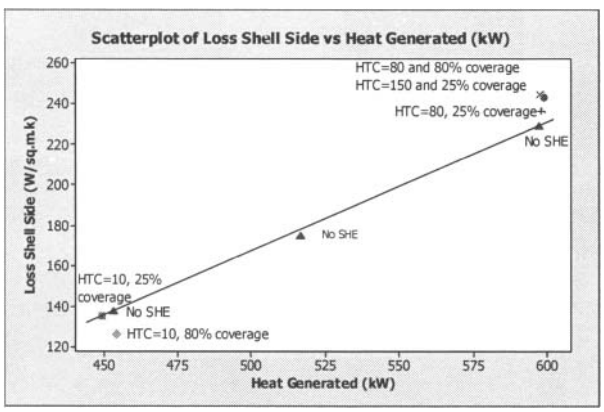

Figure 10. Impact of SHE Configuration on Side Heat Loss

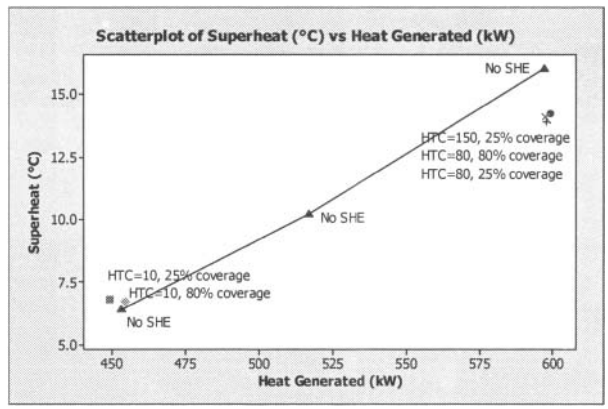

Figure 11. Impact of SHE configuration on superheat

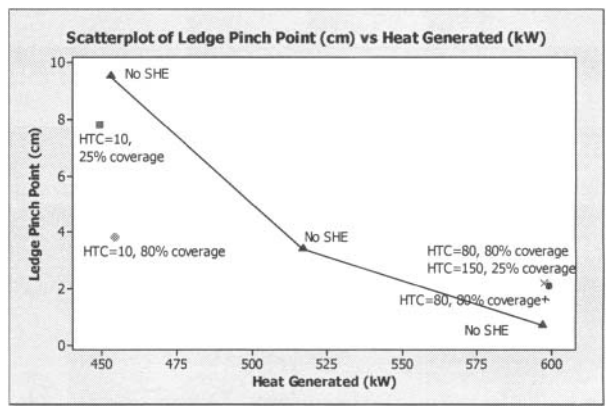

Figure 12. Impact of SHE configuration on ledge pinch point

It can be seen that the heat flux through the sidewall is manipulated by the Shell Heat Exchanger configuration. This results in significant changes of the ledge profile and superheat inside the cell.

Higher heat flux and ledge thickness can be achieved with increased air flow through the SHE or by increasing the area covered by the exchangers but the effect on the ledge is small. Although the heat loss with the SHE in insulation mode changes only through coverage, the impact on the ledge thickness is large.

In contrast, the impact on the bath superheat appears to be limited in insulation mode, while the effect in cooling mode seems constant and attributed to the presence of the Shell Heat Exchangers, with no further decrease in superheat at higher flow or coverage.

Conclusions

This paper demonstrated that the Shell Heat Exchangers designed by the Light Metals Research Centre, through air flow variation and the use of proprietary turbulence promoters, are effective in manipulating the heat transfer coefficient at the pot shell, from 10 to more than 180 W/m^2.K.

With SHE's operated in insulating mode, an average shell temperature increase of up to 75°C was achieved. When cooling was applied, a peak sidewall temperature reduction of up to 200°C

was obtained and the cooling was controlled by adjusting the extraction fan speed. The temperature of the exit air measured was 170 to 200°C, corresponding to a heat content of 9-10 kW per cradle position. The heat transfer coefficients measured for the SHE were 1.5 to 2.5 times higher than that predicted for forced convection through a duct of same dimensions, due to the turbulence promoters used in the SHE.

SHE operation enables a fast readjustment of the cell heat balance by controlling the heat loss from the shell, suitable to counter-balance major power input variation to the cell. It results in an increased window of power modulation, in which a given electrolysis cell can operate stably over time. The power modulation window was shown to be doubled with the use of the shell heat exchangers

The next step of work in regards to the operation of SHE for power modulation involves confirmation of the benefits in operating cells and a study of the slowed dynamic response when using Shell Heat Exchangers.

Acknowledgement

The authors would like to acknowledge the essential contribution of David Cotton and Dr. Ronny Etzion to the experimental work, as well as Dr. Jianning Tang to the thermo-electric modelling.

References

[1] AME Smelter Cost Curve, 2009
[2] Feng N., Tian Y., Peng, J., Wang Y, Qi X., Tu G., "New Cathodes in Aluminum Reduction Cells", Light Metals, 2010
[3] European Energy Exchange, www.eex.com
[4] Eisma D., Patel P., "Challenges in Power Modulation", Light Metals,2009
[5] Taylor M.P., Liu X., Fraser K.J. and Welch B.J., The Dynamic and Performance of Reduction Cell Electrolytes, Light Metals 1990
[6] Namboothiri S., Lavoie P., Cotton D. and Taylor, M.P., "Controlled Cooling of Aluminium Reduction Cell Sidewalls Using Heat Exchangers Supplied with Air, Light Metals 2009
[7] Haugland E., Borset H., Gikling H. and Hoie H., "Effects of Ambient Temperature and Ventilation on Shell Temperature Heat Balance and Side Ledge of an Alumina Reduction Cell", Light Metals 2003
[8] Perry R.H., Green D.W. and Maloney J.O., "Perry's Chemical Engineering Handbook", 6th ed. 1984, USA: Mc Graw-Hill chemical engineering series
[9] Sutherland W.A., "Improved Heat Transfer Performance With Boundary - Layer Turbulence Promotors, Int. J. Hear Mass Transfer Vol. ICI, pp. 1589-1599, Pergamon Press Ltd. 1967
[10] Hung Y. H. and Lin H.H., "An Effective Installation of Turbulence Promoters for Heat Transfer Augmentation in a Vertical Rib-Heated Channel, International journal of heat and mass transfer Vol. 35. No. 1, pp. 2942, 1992